FEL

Asymmetric Reactions of Amino-Acids and Their Precursor Molecules by Circularly Polarized Light from Free Electron Laser

P. K. Sarker[1], T. Kaneko[1], K. Kobayashi[1], J. Takahashi[2], H. Mita[3], M. Adachi[4], H. Zen[4], M. Hosaka[5] and M. Katoh[4]

[1]*Yokohama National University, Yokohama 240-8501, Japan*
[2]*NTT Microsystem Integration Laboratories, Atsugi 243-0198, Japan*
[3]*Fukuoka Institute of Technology, Fukuoka 811-0295, Japan*
[4]*UVSOR Facility, Institute for Molecular Science, Oakazaki 444-8585, Japan*
[5]*Nagoya University, Nagoya 464-8601, Japan*

Introduction

The origin of homochirality in terrestrial biological molecules (dominant L-body amino acids and D-body sugars) remains an unresolved important problem in the study for the origins of life. One of the most attractive hypotheses for the origin of homochirality is nominated as "Cosmic Scenario"; some chiral impulses from asymmetric excitation sources in space triggered asymmetric reactions on the surfaces of such space materials as meteorites or interstellar dusts. According to this scenario, the enantiomeric excesses in terrestrial amino acids can be advocated that asymmetric reactions of complex organic molecules including amino acid precursors were induced by circularly polarized light (CPL) from synchrotron radiation (SR) source in space prior to the existence of terrestrial life. Recently, a wide-field and deep near-infrared circularly polarized light has been observed in the Orion nebula, where massive stars and many low-mass stars are forming [1]. This observation result strongly support the "Cosmic Scenario" with CPL in space for the origin of homochirality in terrestrial bioorganic compounds.

Presently, we are conducting verification ground experiments for the extraterrestrial scenario by using CPL from SR facilities as a simulating polarized energy source. We have already reported the experimental results of asymmetric reactions in solid films of racemic mixtures of amino acids by irradiating them with CPL in ultraviolet (UV) region from free electron laser (FEL) of UVSOR [2]. The emergence of optical anisotropy in the irradiated films was detected by measurements of circular dichroism (CD) spectra. These results have suggested that the UV-CPL irradiation caused not only preferential photolysis between enantiomers but also asymmetric reactions including conformation changes or some other construct distortions. We have carried out UV-CPL irradiation experiments for aqueous solution of amino acids (DL-isovaline and DL-histidine) and for the films of the precursor molecules of amino acids, such as hydantoins (five-membered heterocyclic molecules).

Experimental

Aquesous solution of IVal, His, or copper complex of His (*pH* = 3, 7 or 11 in all cases) was irradiated with CPL-UV at 215 nm from an FEL of UVSOR-II (IMS, Japan). Amino acids were determined by ion-exchange HPLC (Shimadzu LC-10A). Enantiomers of amino acids were separated by HPLC with a chiral column (Sumichiral OA-50000).

Vacuum-evaporated thin film of hydantoin (5, 5-dihydrogen; Fig. 1) was also irradiated with CPL-UV: hydantoin is an achiral molecule and a precursor of glycine. After the irradiation, optical anisotropy of the resulting thin films were observed with circular dichroism (CD) spectra.

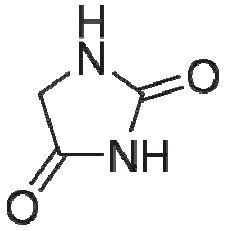

Fig. 1. Hydantoin

Results and Discussion

After R-CPL irradiation of DL-isovaline aqueous solution, small D-excess was observed, and the L-CPL irradiation caused L-excess. Amino acid analysis showed that the major amino acid product from isovaline was alanine.

Achiral hydantoin has presented apparent optical anisotropy in the CD spectra of the irradiated films, suggesting that asymmetric reactions peculiar to the heterocyclic ring molecules can induce chiral constructions in the starting achiral molecules.

These results suggest that UV-CPL played an important role to produce homochirality of terrestrial amino acids from their precursor molecules. Additional experiments for both chiral and achiral hydantoins and analyses including both identification of reaction product molecules and theoretical calculation of photo-induced constructions are important for the solution of the origins of biological homochirality.

[1] T. Fukue *et al.*, Orig. Life Evol. Biosph. **40** (2010) 335.
[2] J. Takahashi *et al.*, Int. J. Mol. Sci. **10** (2009) 3044.

BL2B

Effect of the Magic Number "60" on the Photodissociation Process of C_{70}

H. Katayanagi[1,2] and K. Mitsuke[1,2]

[1]*Dept. of Photo-Molecular Science, Institute for Molecular Science, Okazaki 444-8585, Japan*

[2]*Graduate University for Advanced Studies, Okazaki 444-8585, Japan*

We have developed a photofragment imaging spectrometer suitable for synchrotron radiation (SR) excitation of gaseous molecules of refractory materials [1]. Using this apparatus we have observed the scattering distributions of the fragments produced by the photodissociation of C_{60} such as C_{60-2n}^{2+} [2]. We found that the kinetic energy release (KER) of the reaction step to produce C_{50}^{2+} fragments was smaller than those of the other reaction steps. This shows that the C_{50}^{2+} fragment is more stable than the other C_{60-2n}^{2+} fragments. The relative stability of the fragments can thus be obtained. In the present study, we apply this method to observe fragments produced by the photodissociation of the higher fullerene, C_{70}, which decays into C_{60} fragments through stepwise C_2 emission.

The experiments were performed at BL2B in UVSOR. The experimental procedure is almost identical to that of the photofragment imaging of C_{60} [2].

Figure 1 shows two-dimensional (2D) maps of time-of-flight (TOF, *t*) and arrival position along *y*-direction of ion signals on a position sensitive detector (PSD). The *y*-direction on the figure is orthogonal to the path of the parent C_{70} beam. The conspicuous three spots in Fig. 1 (a) are ascribable from left to right to the parent ions of C_{70}^{3+}, C_{70}^{2+} and C_{70}^{+}, respectively. These spots have narrow *y*-distributions since the C_{70} neutral beam is well collimated. In Figs. 1 (b) and (c) subtle stripes with much broader *y*-distributions are seen on the left of the parent ions' spots; these stripes are assigned to the fragments produced by successive ejection of C_2 units from the parent ions. The broader *y*-distributions of the stripes indicate larger velocity, or higher translational temperatures of the fragments acquired by the dissociation than those of the parent ions.

Figure 2 shows the translational temperatures, *T*, of the fragments determined from the *y*-distributions of the fragments on Fig. 1. The smaller fragments have the higher temperatures. We can regard the gap between curves of $n = 4$ and 5 are smaller than the other gaps between the curves. This means that the temperature increase between C_{62}^{2+} ($n = 4$) and C_{60}^{2+} ($n = 5$) is exceptionally smaller than those between other fragments. The small increase in the C_{60}^{2+} production process reflects small KER in this reaction step. This is partly because of relative stability of C_{60}^{2+} fragment having the magic number of 60. In addition, there might be another reaction pathway to produce C_{60}^{2+} such as one-step two-fragment fission.

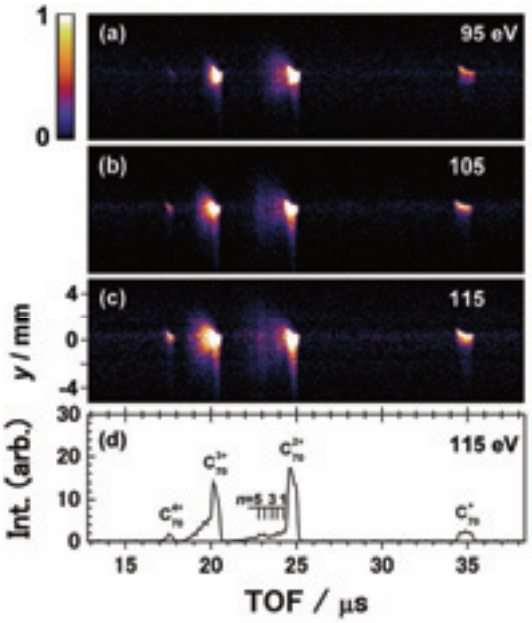

Fig. 1. (a-c) *y*-*t* maps of parent and fragment ions produced by the photodissociation of C_{70}. Excitation photon energies are shown in each panel. (d) TOF profile obtained from (c) by integration with respect to *y*. Assignments of peaks are shown in the panel.

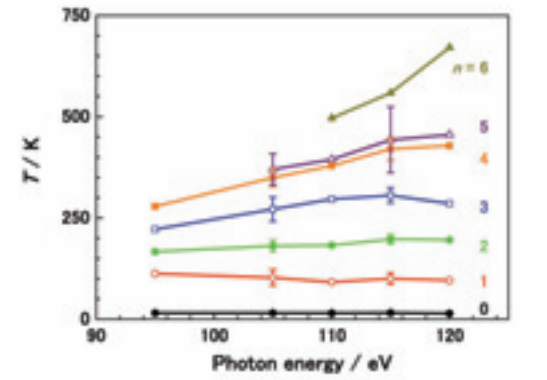

Fig. 2. Excitation photon energy dependence of translational temperatures of parent and fragment ions produced at *n*-th reaction step to produce C_{70-2n}^{2+} evaluated from *y*-*t* maps shown in Fig. 1 (a-c). Error bars show deviations among experimental runs on different days.

[1] Md. S. I. Prodhan *et al.*, Chem. Phys. Lett. **469** (2009) 19.

[2] H. Katayanagi and K Mitsuke, J. Chem. Phys. **133** (2010) 081101.

BL2B

Mass-Analyzed Velocity Map Imaging of Thermal Photofragments from C_{60}

H. Katayanagi[1,2] and K. Mitsuke[1,2]

[1]*Dept. of Photo-Molecular Science, Institute for Molecular Science, Okazaki 444-8585, Japan*

[2]*Graduate University for Advanced Studies, Okazaki 444-8585, Japan*

Dissociation mechanisms of fullerenes have been extensively studied since the fullerenes are systems which have well-defined, highly-symmetric molecular structure despite their large number of degrees of freedom, F (e.g. C_{60}, F = 174). The knowledge on the dissociation mechanisms of such large F systems provides a severe benchmark for various statistical theories of reaction dynamics. In the present study, the velocity distributions of the fragments produced by dissociative photoionization of C_{60} have been measured in the extreme UV region for the first time, using a flight-time resolved velocity map imaging technique combined with a high-temperature molecular beam and synchrotron radiation [1]. From the velocity distributions, detailed properties reflecting the dissociation mechanism can be obtained such as kinetic energy release (KER) of dissociation and partitioning of internal energies of reactants among the degrees of freedom.

The experiments were performed at BL2B in UVSOR. Fullerene (C_{60}) powder was loaded in a quartz tube and heated up by an electric heater at around 700-800 K in vacuum. The C_{60} vapor passed through two apertures and reached the ionization region, where the C_{60} molecular beam (x axis) intersected the monochromatized synchrotron radiation (y axis) at right angles. Ions produced at the ionization region were extracted by a velocity map imaging electrode assembly and projected along z axis on to a position sensitive detector (PSD) of 40 mm in diameter and 375 mm away from the ionization region. Photolectrons were extracted to the opposite direction to the ions and detected by a microchannel plate (MCP) detector. Time of flight (TOF, t) and arrival position (x, y) of ions on the PSD were recorded using the signal of photoelectrons as a start trigger. Three-dimensional (3D) lists of data, (x, y, t), were thus obtained.

Integration of the 3D listdata with respect to x, 2D y-t distributions were obtained (not shown here, see Ref. 1). Further integration with respect to y gives us ordinary TOF profiles. Distributions along y-direction on the y-t map with limited TOF ranges which correspond to mass-to-charge ratios (m/z) of each fragment were then extracted. The y-distribution of each fragment is 1D projection of 3D velocity distribution and is converted to translational temperature.

Figure 1 shows the translational temperatures of the fragments. From the temperatures, average KER for respective reaction steps were obtained assuming stepwise C_2 emission and shown in Fig. 2.

In Fig. 2, the values of KER in the first to fourth steps increase with increasing $h\nu$, reflecting statistical redistribution of the excess energy in the transition state, whereas that in the fifth step leading to C_{50}^{2+} was exceptionally small. This might reflect C_{50} has a cage structure and the number 50 is a magic number although C_{50} cannot satisfy the isolated pentagon rule. In addition, knowledge on the energy partitioning can be obtained from the KER curves. We can estimate the internal energies, E_{int}, of parent C_{60}^{2+} ions from the excitation photon energy, ionization potential and thermal energy of the parent ion. The dashed line in Fig. 2 shows the internal energy divided by the degree of freedom, E_{int} / F. The KER values of n=1 agree with the dashed line. This means that the internal energy partitioned to one degree of freedom is dissipated to the reaction coordinate of C_2 emission among the vibrational degrees of freedom.

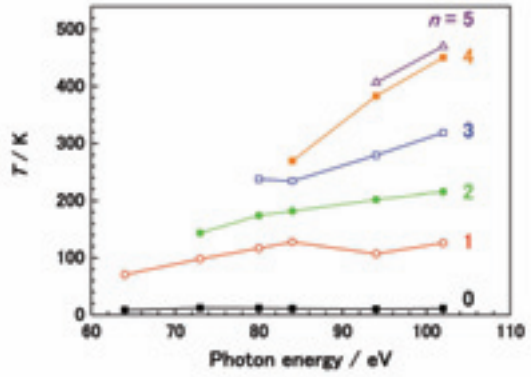

Fig. 1. Excitation photon energy dependence of translational temperatures of the fragments (C_{60-2n}^{2+}).

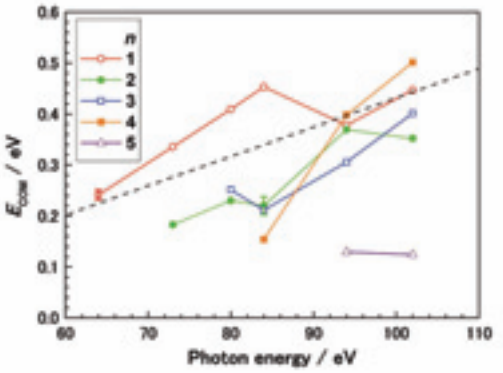

Fig. 2. Excitation photon energy dependence of total average KER generated at the n-th reaction step to produce C_{60-2n}^{2+}. Error bars show the uncertainty caused in the fitting procedure. Dashed line indicates the value of E_{int} / F in the first reaction step.

[1] H. Katayanagi and K Mitsuke, J. Chem. Phys. **133** (2010) 081101.

BL2B

Breakdown Pathways of Doubly-Charged Perfluorocyclobutane and *cis*-1,1,2,2,3,4-Hexafluorocyclobutane

K. Okada[1], T. Nakashima[1], M. Sakai[1], A. Suemitsu[1], H. Katayanagi[2,3] and K. Mitsuke[2,3]
[1]*Department of Chemistry, Hiroshima University, Higashi-Hiroshima 739-8526, Japan*
[2]*Institute for Molecular Science, Okazaki 444-8585, Japan*
[3]*Graduate University for Advanced Studies, Okazaki 444-8585, Japan*

Molecular photoionization and ionic fragmentation processes are of fundamental importance in the upper-atmospheric chemistry and plasma physics. Perfluorocyclobutane (*c*-C_4F_8) is extensively used as a reagent for dry etching of semiconductors. However, the use of the gas in industry has atmospheric implications for global warming. In our previous study [1] we report yield spectra of the fragment ions of *c*-C_4F_8 and *cis*-1,1,2,2,3,4-hexafluorocyclobutane (*cis*-*c*-$C_4H_2F_6$), a candidate for replacing *c*-C_4F_8, in the photon energy range of 25–170 eV. Due to the shortage of the knowledge of the photochemical process, ion pairs originating from charge separation of the multiply-charged molecular ions were detected in this study using a photoelectron–photoion–photoion coincidence (PEPIPICO) technique to obtain information on the breakdown pathways.

The experiments have been performed on the beamline BL2B at the UVSOR facility. The experimental setup has been described in a previous paper [1]. Electrons and ions produced by the photoabsorption were extracted toward the opposite directions. The detection signals of the electrons and ions were fed into the start and stop pulse inputs of a multi-stop time-to-digital converter (FAST ComTec, P7888), respectively, to record time-of-flight (TOF) data. The data were acquired at 35.0, 40.0, 45.0, 50.0 and 90.0 eV. PEPIPICO spectra were constructed from the ion–ion coincidence events as maps.

Figure 1 depicts a typical PEPIPICO spectrum obtained for *c*-C_4F_8 at the excitation energy of 45.0 eV. Several coincidence islands can be found in the spectrum, along with ridges arising from false coincidences. In this study we focus on the slopes of the islands. The coordinate tells us the masses of the two fragment ions, while the slope gives information about the fragmentation mechanism to produce such ions.

The most abundant fragment ion pair detected is $C_2F_4^+/CF^+$. Its coincidence island has round shape, indicating that the ion pair can be formed by some decomposition processes. A long parallelogram of slope –1.01 is observed for the island corresponding to the $C_3F_5^+/CF_2^+$ ion pair. This can be explained by the two-body fragmentation of $C_4F_7^{2+}$. The measured slope for the $C_2F_4^+/CF_2^+$ coincidence island is –1.63, which is well described by the three-body secondary decay mechanism:

$$C_4F_7^{2+} \rightarrow C_2F_4^+ + C_2F_3^+,$$
$$C_2F_3^+ \rightarrow CF_2^+ + CF.$$

In this way, the following breakdown pathways can be identified for *c*-C_4F_8:

$$c\text{-}C_4F_8^{2+} \rightarrow C_4F_7^{2+} + F \rightarrow C_3F_5^+ + CF_2^+ + F \quad (1)$$
$$\rightarrow C_2F_4^+ + C_2F_3^+ + F$$
$$\downarrow$$
$$C_2F_4^+ + CF_2^+ + CF + F \quad (2)$$
$$C_4F_6^{2+} + 2F \rightarrow C_3F_4^+ + CF_2^+ + 2F \quad (3)$$
$$\downarrow$$
$$C_3F_3^+ + CF_2^+ + 3F \quad (4)$$
$$c\text{-}C_4F_8^{2+} \rightarrow C_3F_6^{2+} + CF_2 \rightarrow C_2F_4^+ + CF_2^+ + CF_2$$
$$\downarrow$$
$$CF_3^+ + CF_2^+ + CF_2 + CF \quad (5)$$

etc.

Similar breakdown pathways are found for the fragmentation of *cis*-*c*-$C_4H_2F_4$. Reaction channels deduced from the slope analysis correspond to Reactions 1, 2, 4 and 5, with formally replacing one or two F atoms with H atoms.

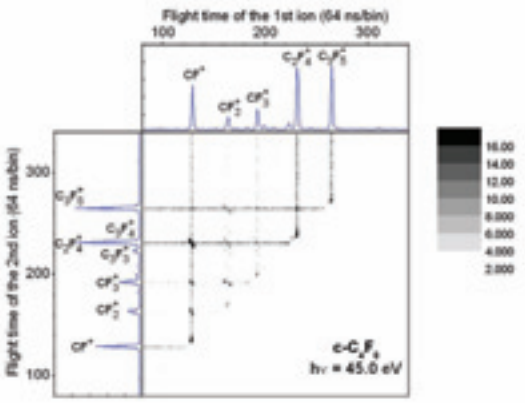

Fig. 1. Overview of a typical PEPIPICO map for *c*-C_4F_8 acquired at 45.0 eV. The top and left panels indicate the corresponding TOF spectrum.

[1] K. Okada, T. Nakashima, M. Sakai, A. Suemitsu, C. Huang, H. Yagi, H. Katayanagi, K. Mitsuke and K. Tabayashi, J. Phys. Conf. Ser., accepted.

BL3U

Electronic Structure of Liquid Methanol Studied by Carbon K-Edge Soft X-Ray Absorption Spectroscopy

M. Nagasaka and N. Kosugi
Institute for Molecular Science, Myodaiji, Okazaki 444-8585, Japan

Methanol (CH_3OH) is a liquid at room temperature and is the simplest of the amphiphilic molecules with both hydrophilic and hydrophobic groups. It is known that some mixtures of methanol and water show characteristic hydrogen bonding networks by the cluster formation [1]. The microscopic structure of the hydrogen bonding network of liquid methanol is not fully understood. X-ray absorption spectroscopy (XAS) is a promising method to study the local electronic structure of the hydrogen bond in liquid water [2] and so on. Combination of the O and C K-edge XAS spectra of methanol is useful to reveal the local electronic structures around C and O atoms separately. Wilson et al. reported XAS spectra of methanol in the total electron yield of liquid microjet of methanol [3]. It is difficult to extract liquid XAS spectra from the spectra of gas and liquid mixture. Recently, we have developed a liquid cell for the measurement of XAS in the transmission mode [4]. In the present work, we apply this transmission C K-edge XAS technique to investigate the local electronic structure of liquid methanol.

The experiments were performed at BL3U. The liquid thin layer was sandwiched between two 100 nm-thick SiN*x* (NTT AT Co.). Thickness of the liquid layer was optimized to be 250 nm by adjusting the helium backpressure. The energy resolution was set to be 0.19 eV at 280 eV. The photon energy was calibrated by the C 1s - π* peak (290.77 eV) of the CO_2 gas mixture in He [5]. XAS spectra for methanol gas mixture in He were also measured.

Figure 1 shows C K-edge XAS spectra of molecular (gas) and liquid methanol at 25 ºC. Two peaks around 288 and 289.5 eV and several Rydberg states are observed in the molecular spectra. The 288 eV and 289.5 eV peaks contain O-H and C-H components and the 292.5 eV peak contains a σ* C-O component. Our C K-edge XAS spectrum of liquid methanol shows a simple structure with three contributions around 288.5, 290, and 293 eV as shown in Fig. 1(b); on the other hand, the microjet experiment did not give such a large spectral difference between gas and liquid [3]. The XAS spectra for methanol clusters [6] are similar to our liquid spectrum. The contribution from the methanol gas would be not completely removed in the microjet experiments.

As shown in Fig. 1 (b), the peak around 288.5 eV in liquid methanol is shifted to higher photon energy compared to that of methanol gas. The energy shift (0.53 eV) would be caused by the formation of the hydrogen bonding networks between methanol molecules. The peak around 290 eV in liquid methanol is also shifted to the higher photon energy compared to that of methanol gas, but the energy shift (0.20 eV) is smaller than in the first peak. This may be explained by a dominant contribution from the hydrophilic OH component in the first band and a dominant contribution from the hydrophobic CH component in the second peak. The peak around 293 eV does not show a noticeable difference between gas and liquid because the σ* (C-O) orbital is not influenced by the hydrogen bonding network.

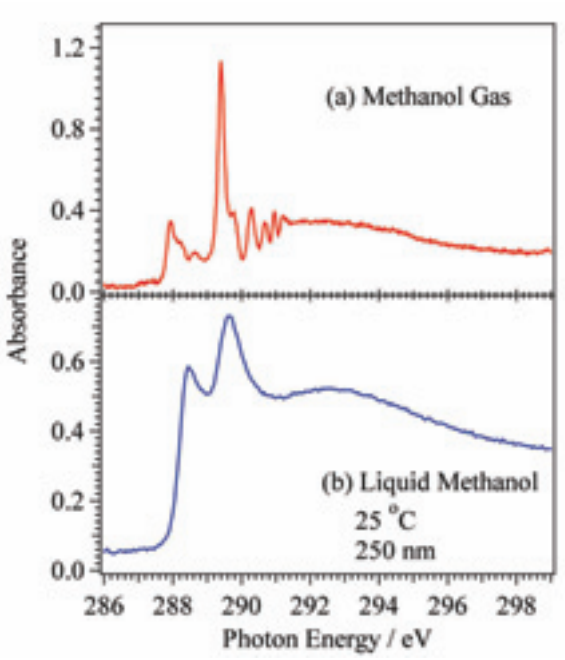

Fig. 1. Carbon K-edge XAS spectra for (a) methanol gas and (b) liquid methanol at 25 ºC. The thickness of liquid methanol layer is estimated to be 250 nm.

[1] C. Corsaro *et al.*, J. Phys. Chem. B **112** (2008) 10449.
[2] Ph. Wernet *et al.*, Science **304** (2004) 995.
[3] K. R. Wilson *et al.*, J. Phys. Chem. B **109** (2005) 10194.
[4] M. Nagasaka *et al.*, J. Electron Spectrosc. Relat. Phenom. **177** (2010) 130.
[5] T. Tanaka *et al.*, Phys. Rev. Lett. **95** (2005) 203002.
[6] Y. Tamenori *et al.*, J. Chem. Phys. **128** (2008) 124321.

BL3U

Hydration Structures of Li Cations in LiCl Aqueous Solutions Studied by Oxygen K-Edge Soft X-Ray Absorption Spectroscopy

M. Nagasaka[1], T. Hatsui[2] and N. Kosugi[1]

[1]*Institute for Molecular Science, Myodaiji, Okazaki 444-8585, Japan*

[2]*XFEL Project Head Office, RIKEN, Sayo-cho, Hyogo 679-5148, Japan*

Macroscopic properties of aqueous solutions, such as viscosity, boiling point, and freezing point, are influenced by the interaction between ions and water molecules because the hydrogen bonding networks are formed or broken by the interaction of the ions. In aqueous salt solutions, the cation is near the oxygen site of water molecules, whereas the anion is near the hydrogen site. The interaction of the anion with water has been studied by using the OH stretch vibration mode in the Raman spectroscopy [1]. On the other hand, the hydration of the cation has not been studied in detail by vibrational spectroscopies because the OH vibration is insensitive to the cation. Recently, the electronic structure of liquid water has been studied by oxygen K-edge X-ray absorption spectroscopy (XAS) [2]. The pre-edge peak of liquid water (535 eV) corresponds to the transition from the oxygen 1s electron to the $4a_1$* unoccupied orbital, which is mainly distributed on the oxygen atom and is dominated by the short-range interaction. The energy shift of the pre-edge peak would be sensitive to the nearest neighbor cation coordination to the water oxygen. In this work, we have studied the hydration shell of Li cations in the LiCl aqueous solutions by using oxygen K-edge XAS.

The experiments were performed at BL3U. The details of the liquid cell for the XAS measurements in the transmission mode were described previously [3]. The liquid thin layer was sandwiched between two 100 nm-thick SiN*x* (NTT AT Co.). The thickness of the liquid layer was optimized from 50 to 1000 nm by changing the He backpressure [3]. The photon energy was calibrated by the O 1s - π* peak (530.8 eV) of the O_2 gas mixture in He.

Figure 1 shows O K-edge XAS spectra for the LiCl aqueous solutions with different concentrations at 25 ºC. As the concentration increases, the pre-edge peak is gradually shifted to the higher photon energy. As shown in the inset, the isosbestic points were observed in the pre-edge region, which suggests the existence of two components in the pre-edge region dominated by the short-range interaction. We also measured the O K-edge XAS for different cations and anions (NaCl, KCl, NaBr, and NaI); the energy shift of the pre-edge region is dependent on the alkali ion but is not on the halide ion. This indicates that the two components in the spectra (Fig. 1) are derived from the bulk water and the Li^+-solvating water.

In order to extract the contribution of the Li^+-solvating water from the spectra, the numbers of the bulk and solvating water molecules were calculated, assuming the coordination number of water molecules to Li^+ is 4 [4]. In the XAS spectra for the nearest neighbor water solvating the different cations, the pre-edge peak in the Li ion shows a larger energy shift than in the Na and K ions. The neutron diffraction studies showed that the bond between the Li cation and water is 0.190 nm, which is shorter than those of the Na and K ions [4]. This indicates that the pre-edge peak shift arises from the nearest-neighbor interaction of the cation with the oxygen site of solvating water molecules and the hydration to the Li ion is stronger than the Na and K ions.

We also measured O K-edge XAS for the LiCl aqueous solutions with different temperatures (4, 25, and 60 ºC); the pre-edge peak corresponding to the Li^+-solvating water is not shifted irrespective of the temperature. This agrees that the interaction of the Li ion with liquid water is strong enough to keep the hydration shells even in different temperatures.

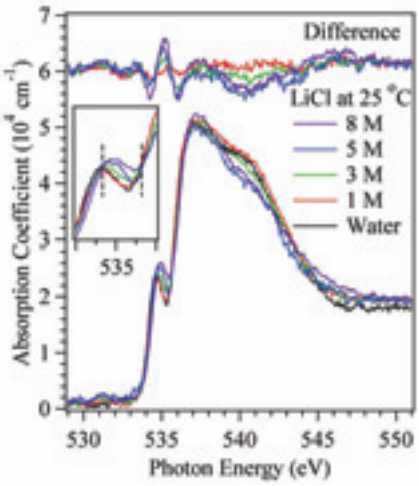

Fig. 1. Oxygen K-edge XAS spectra for the pure water and the LiCl aqueous solutions with different concentrations at 25 ºC. The spectral differences between aq. LiCl and bulk water are also shown. The inset shows isosbestic points (dashed lines) in the pre-edge region.

[1] J. D. Smith *et al.*, J. Am. Chem. Soc. **129** (2007) 13847.

[2] L.-Å. Näslund *et al.*, J. Phys. Chem. A **109** (2005) 5995.

[3] M. Nagasaka *et al.*, J. Electron Spectrosc. Relat. Phenom. **177** (2010) 130.

[4] N. Ohtomo and K. Arakawa, Bull. Chem. Soc. Jpn. **52** (1979) 2755.

BL3U

Structures of Small Mixed Argon-Nitrogen Clusters Studied by Soft X-Ray Photoelectron Spectroscopy

M. Nagasaka[1], E. Serdaroglu[2], R. Flesch[2], E. Rühl[2] and N. Kosugi[1]
[1]*Institute for Molecular Science, Myodaiji, Okazaki 444-8585, Japan*
[2]*Physikalische Chemie, Freie Universität Berlin, Takustr. 3, D-14195 Berlin, Germany*

The structure of heterogeneous clusters is dependent on the cluster size and composition. The structure of small clusters is very important from the viewpoint of the cluster formation mechanism. The cluster structures have been extensively investigated by theoretical simulations [1]; on the other hand, there are few experiments to study the structures of small mixed clusters because of several experimental difficulties. Recently, we have measured X-ray photoelectron spectroscopy (XPS) of small homogeneous Kr and Xe clusters [2, 3] and small mixed Kr-Xe clusters. Different binding energy shifts in the Kr 3d and Xe 4d edges, which are observed in different sites of the Kr-Xe mixed clusters. These arise from the two different induced polarization effects of surrounding Kr and Xe atoms. In the present study, we have investigated the structures of small mixed Ar-N_2 clusters of different composition by analyzing the core level shifts. N_2 is a linear molecule. Therefore, the core level shift of mixed Ar-N_2 clusters would be influenced by anisotropic interactions of the N_2 molecules.

The experiments were performed at BL3U. The mixed Ar-N_2 clusters were formed in a supersonic expansion of the gas mixtures containing an Ar mixing ratio between 10 % and 40 %. The nozzle temperature and gas pressure were 163 K and 0.5 MPa, respectively. The average size of the homogeneous Ar clusters becomes 200, as estimated from the expansion conditions.

Figure 1 shows the Ar $2p_{3/2}$ XPS spectra for the Ar cluster and the mixed Ar-N_2 clusters of different composition. The surface and bulk sites of the clusters are distinguished by a fitting procedure, as shown in Table 1. The cluster size of 200 corresponds to icosahedral multilayer structures with 4 or 5 layers. The intensity ratio of the surface and bulk sites observed for the Ar $2p_{3/2}$ XPS spectra of the pure (100 %) Ar_{200} cluster is consistent with such icosahedral multilayer structures. On the other hand, in the expansion containing 10 % Ar, the intensity of the surface sites is smaller than that of the bulk sites. This intensity ratio suggests a core-shell structure, where the Ar aggregates are located in the bulk and are covered by a N_2 shell. We have roughly estimated the composition of N_2 bound in clusters from the partial pressure of N_2, and confirmed that the surface-to-bulk ratio of Ar is consistent with a core-shell structure, where Ar is covered by the N_2. These core-shell structures are also observed in expansions containing 20 % and 40 % Ar.

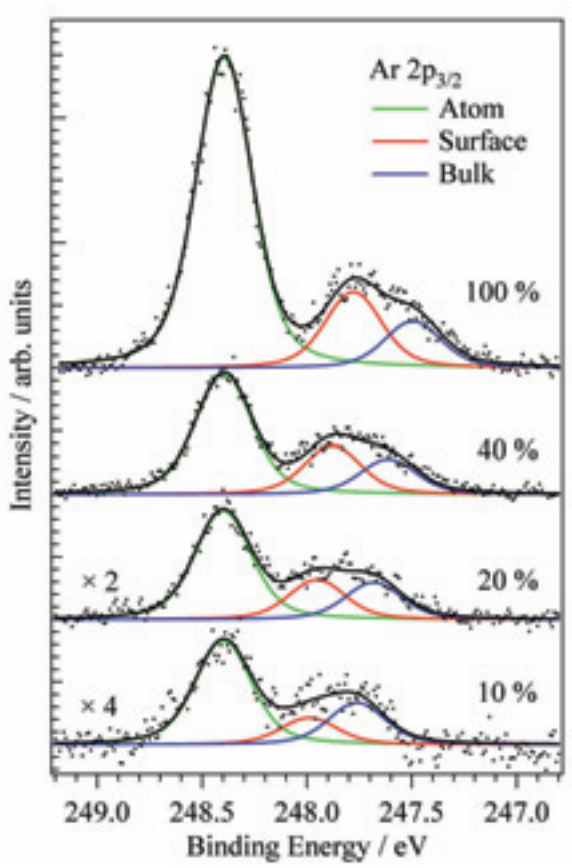

Fig. 1. Ar $2p_{3/2}$ XPS spectra of mixed Ar-N_2 clusters prepared from different mixing ratio of Ar. The surface and bulk sites of the mixed clusters are obtained from a fitting procedure.

Table 1. Binding energy shifts in the Ar $2p_{3/2}$ regime at different sites of the mixed clusters relative to the atomic value in eV. The values in parentheses correspond to the relative intensities of the Ar atoms.

Ar (%)	Surface	Bulk
100	-0.62 (124)	-0.90 (76)
40	-0.52 (79)	-0.79 (57)
20	-0.45 (32)	-0.72 (30)
10	-0.41 (11)	-0.64 (17)

[1] For example, J. W. Hewage and F. G. Amar, J. Chem. Phys. **119** (2003) 9021.
[2] T. Hatsui *et al.*, J. Chem. Phys. **123** (2005) 154304.
[3] M. Nagasaka *et al.*, J. Electron Spectrosc. Relat. Phenom. **183** (2011) 29.

BL6U

Chemical Environment Effect on Doubly Charged Ion States after Auger Decay of Ethyl Trifluoroacelate Molecules

H. Iwayama[1], E. Shigemasa[1] and P. Lablanquie[2]
[1]*UVSOR Facility, Institute for Molecular Science, Okazaki 444-8585, Japan*
[2]*LCPMR, Université Pierre et Marie Curie, 75231 Paris Cedex 05, France*

Inner-shell photoionization of light elements is generally accompanied by an Auger decay process. A photoelectron and Auger electron are thus ejected, and a doubly charged ion is produced. The binding energy of an inner-shell electron in a molecule depends not only on the atomic energy level but also its chemical environment, which gives rise to a small shift in the energy spectrum. This is the so-called chemical shift. Based on the observation of such chemical shifts in X-ray photoelectron spectra, we can qualitatively discuss chemical bond character and atomic charge in molecules.

The chemical shifts may also be reflected in the binding energies of the doubly charged ion state after Auger decay, because the Auger transition probability depends on a spatial overlap between the inner- and outer-shell electron wavefunctions. In the present work, we investigated the binding energy spectra after Auger decay for ethyl trifluoroacelate molecules ($C_4H_5F_3O_2$) which have four carbon atoms in different chemical environment. This sample was used to demonstrate the importance of chemical shifts in X-ray photoelectron spectra by K. Siegbahn [1].

In order to obtain the binding energy spectra of doubly charged ion states after Auger decay, we performed a high resolution electron spectroscopy on the soft X-ray beamline BL6U at UVSOR. We measured kinetic energies of photoelectrons and Auger electrons of the C1s, O1s and F1s ionizations with a high performance hemispherical electron energy analyzer MBS-A1, developed by the MB Scientific AB company. The photon energies were set at 330, 575 and 730 eV for the C1s, O1s and F1s ionizations, respectively.

Figure 1 shows the C1s photoelectron spectrum, where four peaks corresponding to the four different carbon sites are clearly observed: the chemical shifts in binding energies of the $C1s^{-1}$ states are detected. By varying the photon energy, binding energies of $F1s^{-1}$ and $O1s^{-1}$ states are also determined to be 694 and 539 eV, respectively.

We measured Auger electron spectra for the F1s and O1s ionizations. From the Auger electron spectra and binding energies of the $F1s^{-1}$ and $O1s^{-1}$ states, we obtained binding energy spectra of doubly charged ion states after Auger decay, which are shown in Fig. 2. Here the binding energies for the C_F and C_O sites were measured on the undulator beamline PLÉIADES at SOLEIL with using a magnetic bottle electron spectrometer. We found that the binding energy spectra after the Auger decays of the $F1s^{-1}$ and $O1s^{-1}$ states are close to those for the $C1s^{-1}$ states of the carbon sites neighboring to the F and O atoms, respectively. These results indicate that the doubly charged ion states after Auger decay reflect the chemical environment near the core-shell ionized atoms. Our results suggest that the doubly charged ion states after Auger decay can be also used as a sensitive tool for a chemical analysis.

[1] U. Gelius *et al.,* J. Electron Spectrosc. **2** (1973) 405.

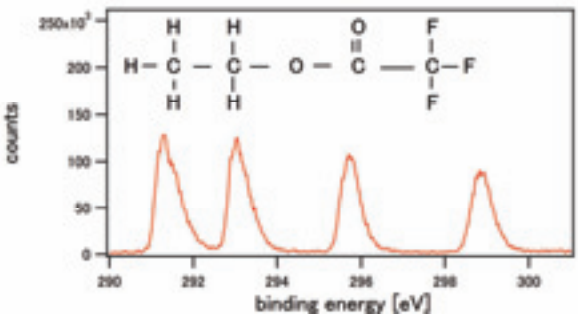

Fig. 1. The chemical shifts in X-ray photoelectron spectrum for ethyl trifluoroacelate. The energy resolutions for the monochromator and analyzer were both set to 30 meV.

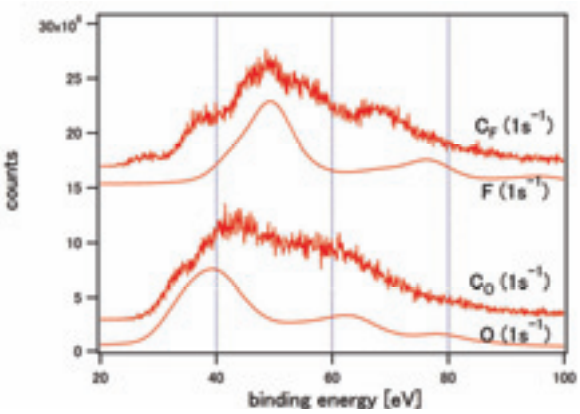

Fig. 2. The binding energy spectra of the doubly charged ion states after Auger decay for the C1s, F1s and O1s ionizations. C_F and C_O denote the carbon atoms neighboring to the F and O atoms, respectively.